University of Groningen

Sodium glucose co-transporter 2 inhibition increases epidermal growth factor expression and improves outcomes in patients with type 2 diabetes

Sen, Taha; Ju, Wenjun; Nair, Viji; Ladd, Patricia; Menon, Rajasree; Otto, Edgar A.; Pyle, Laura; Vigers, Tim; Nelson, Robert G.; Arnott, Clare

IMPORTANT NOTE: You are advised to consult the publisher's version (publisher's PDF) if you wish to cite from it. Please check the document version below.

Document Version
Publisher's PDF, also known as Version of record

[Link to publication in University of Groningen/UMCG research database](#)

Sodium glucose co-transporter 2 inhibition increases epidermal growth factor expression and improves outcomes in patients with type 2 diabetes

Check for updates

OPEN

Taha Sen[1,12], Wenjun Ju[2,3,12], Viji Nair[2], Patricia Ladd[4], Rajasree Menon[2,3], Edgar A. Otto[2], Laura Pyle[5,6], Tim Vigers[5,6], Robert G. Nelson[7], Clare Arnott[8,9], Bruce Neal[8], Michael K. Hansen[10], Matthias Kretzler[2,3,13], Petter Bjornstad[6,11,13] and Hiddo J.L. Heerspink[1,8,13]

[1]Department of Clinical Pharmacy and Pharmacology, University of Groningen, University Medical Centre Groningen, Groningen, The Netherlands; [2]Division of Nephrology, Department of Internal Medicine, University of Michigan, Ann Arbor, Michigan, USA; [3]Department of Computational Medicine and Bioinformatics, University of Michigan, Ann Arbor, Michigan, USA; [4]Department of Radiology, University of Colorado School of Medicine, Aurora, Colorado, USA; [5]Department of Biostatistics and Informatics, Colorado School of Public Health, Aurora, Colorado, USA; [6]Section of Endocrinology, Department of Pediatrics, University of Colorado School of Medicine, Aurora, Colorado, USA; [7]Chronic Kidney Disease Section, National Institute of Diabetes and Digestive and Kidney Diseases, Phoenix, Arizona, USA; [8]The George Institute for Global Health, University New South Wales (UNSW), Sydney, New South Wales, Australia; [9]Department of Cardiology, Royal Prince Alfred Hospital, Sydney, New South Wales, Australia; [10]Janssen Research & Development, LLC, Spring House, Pennsylvania, USA; and [11]Division of Renal Diseases and Hypertension, Department of Medicine, University of Colorado School of Medicine, Aurora, Colorado, USA

Underlying molecular mechanisms of the kidney protective effects of sodium glucose co-transporter 2 (SGLT2) inhibitors are not fully elucidated. Therefore, we studied the association between urinary epidermal growth factor (uEGF), a mitogenic factor involved in kidney repair, and kidney outcomes in patients with type 2 diabetes (T2D). The underlying molecular mechanisms of the SGLT2 inhibitor canagliflozin on EGF using single-cell RNA sequencing from kidney tissue were examined. Urinary EGF-to-creatinine ratio (uEGF/Cr) was measured in 3521 CANagliflozin cardioVascular Assessment Study (CANVAS) participants at baseline and week 52. Associations of uEGF/Cr with kidney outcome were assessed using multivariable-adjusted Cox regression models. Single-cell RNA sequencing was performed using protocol kidney biopsy tissue from ten young patients with T2D on SGLT2i, six patients with T2D on standard care only, and six healthy controls (HCs). In CANVAS, each doubling in baseline uEGF/Cr was associated with a 12% (95% confidence interval 1-22) decreased risk of kidney outcome. uEGF/Cr decreased after 52 weeks with placebo and remained stable with canagliflozin (between-group difference +7.3% (2.0-12.8).

In young persons with T2D, EGF mRNA was primarily expressed in the thick ascending loop of Henle. Expression in biopsies from T2D without SGLT2i was significantly lower compared to HCs, whereas treatment with SGLT2i increased EGF levels closer to the healthy state. In young persons with T2D without SGLT2i, endothelin-1 emerged as a key regulator of the EGF co-expression network. SGLT2i treatment was associated with a shift towards normal EGF expression. Thus, decreased uEGF represents increased risk of kidney disease progression in patients with T2D. Canagliflozin increased kidney tissue expression of EGF and was associated with a downstream signaling cascade linked to tubular repair and reversal of tubular injury.

Correspondence: *Hiddo J.L. Heerspink, Department of Clinical Pharmacy and Pharmacology, University of Groningen, Hanzeplein 1, P.O. Box 30 001, 9700 RB, Groningen, The Netherlands. E-mail: h.j.lambers.heerspink@umcg.nl; or Matthias Kretzler, Department of Medicine/Nephrology, University of Michigan, 1560 MSRB II, 1150 W. Medical Center Drive -SPC5676, Ann Arbor, Michigan 48109, USA. E-mail: kretzler@med.umich.edu; or Petter Bjornstad, Department of Pediatrics and Medicine, 13121 East 17th Avenue, Mailstop 8415 Aurora, Colorado 80045, USA. E-mail: Petter.M.Bjornstad@cuanschutz.edu*

[12]Joint first authors.

[13]Joint senior authors.

Received 18 October 2022; revised 30 June 2023; accepted 21 July 2023; published online 4 August 2023

Sodium–glucose cotransporter 2 inhibitors (SGLT2i) block reabsorption of sodium and glucose in the proximal tubule. Large clinical trials have shown that SGLT2i slow the progression of kidney function decline and reduce the risk of kidney failure in patients with chronic kidney disease (CKD) with and without type 2 diabetes (T2D).[1–4] The mechanisms contributing to these protective effects are understood incompletely, but they likely involve various pathways. including attenuation of intraglomerular hyperfiltration, amelioration of hypoxia, reduction in inflammation metabolic reprogramming promoting autophagy, and mitophagy.[5]

Lay Summary

The underlying mechanism by which sodium glucose co-transporter 2 (SGLT2) inhibitors reduce the risk of kidney failure in patients with type 2 diabetes (T2D) is incompletely understood. In a large clinical trial of patients with T2D, we observed that each increment in urinary epidermal growth factor (EGF) is associated with a lower risk of kidney failure. In kidney biopsies, we observed that EGF expression was significantly lower in young persons with T2D compared with that in healthy controls, whereas EGF expression in young persons with T2D on SGLT2 inhibitors was closer to the level observed in HCs. Collectively, these data support a role for EGF in the kidney-protective effect of SGLT2 inhibitors, and they suggest that EGF may be used as a pharmacodynamic marker of response to SGLT2 inhibition.

Epidermal growth factor (EGF) is a key mitogenic factor involved in cell proliferation, hypertrophy, migration, and differentiation of epithelial cells.[6,7] EGF is produced predominantly in the ascending loop of Henle and the distal convoluted tubule (DCT), and it exerts its effect through binding to the EGF receptor, which is widely expressed in the kidney along the glomerulus, the loop of Henle, the DCT, and the collecting duct.[7] Previous studies have reported decreased excretion of urinary EGF (uEGF) in different kidney pathologies, including in patients with T2D and CKD.[8] Moreover, the EGF level measured in tissue from kidney biopsies of patients correlates with uEGF and is associated with adverse kidney outcomes and kidney disease progression.[7,9] These findings suggest that EGF plays a central role in promoting regenerative responses following kidney injury. However, the effects of SGLT2i on uEGF in clinical studies have yet to be examined.

Accordingly, in this study, we assessed whether baseline uEGF normalized by urine creatinine (uEGF/Cr) is associated with kidney outcomes in patients with T2D at high cardiovascular risk in the Canagliflozin Cardiovascular Assessment Study (CANVAS) trial. Next, we investigated whether the SGLT2i canagliflozin increased the concentration of uEGF/Cr in the CANVAS trial. Finally, we explored the molecular mechanisms for how SGLT2 inhibition might increase uEGF using single-cell RNA sequencing (scRNA-seq) from kidney biopsies from young persons with T2D who were and who were not using SGLT2i from the Renal Hemodynamics, Energetics and Insulin Resistance in Youth Onset Type 2 Diabetes Study (Renal-HEIR) and the Metabolic Surgery on Pancreatic, Renal, and Cardiovascular Health in Youth with Type 2 Diabetes (IMPROVE-T2D) study.

METHODS

Patients and study design of the CANVAS trial

The CANVAS trial was a multicenter, double-blinded, placebo-controlled, randomized clinical trial that assessed the safety and efficacy of the SGLT2i canagliflozin on cardiovascular and kidney outcomes in participants with T2D who were at high cardiovascular risk or had a history of cardiovascular disease. Results of this trial have been reported previously.[2] In brief, the CANVAS trial enrolled 4330 participants from 24 countries. Participants were randomized to 100 mg or 300 mg canagliflozin or matching placebo in a 1:1:1 ratio. The median follow-up duration was 6.1 years. Before trial initiation, all participants were offered the option to participate in the exploratory biomarker research study, in which blood and urine samples of the participants were stored for future biomarker exploratory research. All participants, care providers, trial staff, and outcome assessors were blinded to treatment allocation during the study. Written informed consent was obtained before study initiation. The informed consent for blood and urine collection for biomarker research was separate and optional. The CANVAS trial was conducted following the principles of the Declaration of Helsinki and was registered with ClinicalTrials.gov (Identifier: NCT01032629). The CANVAS trial was approved by an ethics committee at each participating site.

Inclusion criteria for the CANVAS trial were a diagnosis of T2D; an HbA1c level ≥ 58 mmol/mol (7.0%) and ≤ 91 mmol/mol (10.5%); and an age of ≥30 years and a history of symptomatic atherosclerotic cardiovascular disease or an age of ≥50 years with >2 risk factors for cardiovascular disease. These risk factors included a duration of T2D of ≥10 years, systolic blood pressure >140 mm Hg, treatment with >1 antihypertensive agent, current smoking status, diagnosis of micro- or macroalbuminuria, and a high-density lipoprotein cholesterol level of <1 mmol/l. At inclusion, patients also needed to meet other criteria for inclusion, including having an estimated glomerular filtration rate (eGFR) > 30 ml/min per 1.73 m^2. The appendix of the first publication of the CANVAS trial includes the full list of these criteria.

Patients and study design of the biopsy study for EGF scRNA-seq analysis

Adolescents and young adults (N = 16) with youth-onset T2D (12–21 years of age, T2D onset at < 18 years of age, diabetes duration 1–10 years, and HbA1c <11%) from the Renal-HEIR (ClinicalTrials.gov Identifier: NCT03584217) and the IMPROVE-T2D study (ClinicalTrials.gov Identifier: NCT03620773) who underwent an optional research kidney biopsy were included in this analysis. These participants were recruited from the Type 2 Diabetes and Metabolic Bariatric Surgery Clinics at the Children's Hospital Colorado at the Anschutz Medical Campus in Aurora, Colorado. T2D was defined by the American Diabetes Association criteria plus the absence of glutamic acid decarboxylase, islet cell, zinc transporter 8, and/or insulin autoantibodies. The main exclusion criteria for the optional kidney biopsy included the following: evidence of a bleeding disorder or complications from bleeding; use of aspirin, nonsteroidal antiinflammatory drugs (NSAIDs) or other blood thinners that could not be stopped safely for a sufficient time period before and after the biopsy; eGFR < 40 ml/min per 1.73 m^2, single kidney (either by history, or documented by prior imaging or ultrasound performed prior to the biopsy), and uncontrolled or difficult-to-control hypertension (>150/90 mm Hg at day of biopsy).

The Renal-HEIR and IMPROVE-T2D cohorts have intentionally harmonized study protocols and both were approved by the Colorado Multiple Institutional Review Board. Participants and/or parents provided written informed assent and/or consent, as appropriate for age. Participants who opted to undergo the optional kidney biopsy specifically and additionally provided consent to the

research and biopsy teams. Medication use was recorded for all participants, and T2D treatment was prescribed at the discretion of their medical provider. Normative reference tissue was provided by 6 healthy adult participants in the Control of Renal Oxygen Consumption, Mitochondrial Dysfunction, and Insulin Resistance (CROCODILE) study (ClinicalTrials.gov Identifier: NCT04074668).

uEGF assay and scRNA-seq assessment in kidney biopsies

Urine samples for exploratory biomarker research were collected and stored at baseline and week 52 after randomization. For this study, we used the Mesoscale Quickplex SQ 120 platform (Meso Scale Diagnostics), which is a high-performance electro-chemiluminescence immunoassay, to measure EGF in urine. All urine samples were measured between April 2019 and February 2020. In total, 390 of the 3521 urine samples were measured in duplicate. The mean (minimum, maximum) coefficient of variation of the duplicates was 5% (0%, 23%).

To define the RNA expression and regulation patterns of EGF upon SGLT2i treatment, scRNA-seq analysis was performed on cell populations obtained from kidney tissue samples of 10 patients treated with an SGLT2i (9 patients were using canagliflozin, and 1 patient was using empagliflozin), 6 patients under standard care, and 6 healthy reference tissues. Tissue processing, single-cell isolation, and scRNA-seq data generation were performed according to the protocol developed for the Kidney Precision Medicine Project.[10–13] Details of the scRNA-seq analysis across all kidney cell types were reported previously.[14]

Outcomes

CANVAS. The composite kidney outcome was defined as a sustained 40% decline of eGFR or kidney failure defined as an eGFR < 15 ml/min per 1.73 m^2, need for dialysis or kidney transplantation, or death related to kidney disease. The kidney outcome was adjudicated by a blinded adjudication committee using pre-defined and rigorous endpoint definitions.

Statistical analysis

CANVAS clinical trial. Normal distributed continuous variables were reported as means with SDs. Skewed distributed continuous variables were reported as median values with interquartile ranges and underwent natural logarithmic transformation before analyses. Categorical variables were reported as percentages.

The hazard ratios (HRs) for the composite kidney outcome for uEGF/Cr categorized into quartiles, or doubling of uEGF/Cr, were estimated using multivariable Cox proportional hazards regression. Four consecutive models, each built with different covariates, were used to assess the impact of the covariates between uEGF/Cr and the composite kidney outcome. The first model included age, sex, race, and treatment allocation as covariates. We added in the second model the covariates HbA1c, systolic blood pressure, body mass index, low-density lipoprotein, high-density lipoprotein, and the history of cardiovascular disease. In the third model, we added baseline eGFR. Last, the log-transformed urinary albumin-to-creatinine ratio was added to the fourth model. The fully adjusted model also was used to explore the association between uEGF and kidney outcomes in subgroups defined by treatment allocation, baseline age, sex, eGFR, urinary albumin-to-creatinine ratio, and cardiovascular disease history, to assess possible effect modification by these variables.

We assessed whether baseline uEGF/Cr modified the treatment effect of canagliflozin versus placebo on the composite kidney

outcome by fitting Cox proportional hazard regression models. Heterogeneity was tested in the relevant Cox model by adding an interaction term between uEGF/Cr, fitted as a categorical variable into tertiles, and treatment allocation.

The placebo-corrected effect of canagliflozin on uEGF/Cr was calculated by using an analysis of covariance (ANCOVA) model, with the change in uEGF/Cr defined as the outcome, and with treatment allocation and baseline uEGF/Cr as the covariates. This effect was also assessed for the subgroups defined by baseline urinary albumin-to-creatinine ratio and eGFR.

The association of the 1-year change in uEGF/Cr from baseline with subsequent kidney outcomes was assessed using a Cox proportional hazards regression model adopted to a landmark approach. Any kidney outcomes that occurred in the first year were excluded from the analysis. The 1-year change in uEGF/Cr was categorized into quartiles that then were fitted in Cox proportional hazard regression models. The second quartile was taken as a reference to assess the HRs of an increase in uEGF/Cr with a decrease or no change, as this quartile was the change in uEGF/Cr close to 0. The first model included baseline uEGF/Cr, age, sex, race, and treatment allocation. We added the baseline and 1-year change in eGFR to the second model. In the third model, we replaced the baseline and 1-year change in eGFR with the urinary albumin-to-creatinine ratio. The fourth model included all aforementioned covariates. Last, we added history of cardiovascular disease, HbA1c, systolic blood pressure, body mass index, low-density lipoprotein, high-density lipoprotein, and the 1-year change in systolic blood pressure, body mass index, and HbA1c.

Identification of EGF co-regulated gene signatures and pathway identification. ScRNA-seq analysis was performed using the cortex region of the kidney biopsy and processed according to the Kidney Precision Medicine Project single-cell protocol.[10,14–16]

To summarize, single cells isolated from frozen tissues using Liberase TL were processed by the University of Michigan Advanced Genomics Core facility. Standard processing of sample demultiplexing, barcode processing, and quantification were performed using 10X Cell Ranger v6 pipeline from 10X Genomics.[17–19] Ambient mRNA content removal was performed using SoupX and followed further processing with cells having gene counts between 500 and 5000, and <50% mitochondrial genes.[10] Individual sample matrices were combined using RunHarmony in Seurat, version 4.0.0.[10,20,21] Cluster annotation followed the literature-derived kidney markers from previous Kidney Precision Medicine Project publications.[10,21]

Genes that were differentially expressed in *EGF*-expressing (*EGF*+) versus EGF-nonexpressing (*EGF*–) thick ascending loop (TAL) cells from patients with youth-onset T2D with or without SGLT2i treatment were identified using the FindMarkers Seurat function. *EGF*+ versus *EGF*– cells were based on greater than 0 (*EGF* >0) normalized gene expression. For the differential gene signature, the Welch *t* test was used to compare the differences, and genes with Bonferroni-adjusted *P* values <1^{-20} that also had a fold change > 1.20 or < −0.83 were selected.

To determine the significantly enriched biological processes and pathways in the differentially expressed gene sets, we used a method described previously[22] and projected gene signatures that were dys-regulated in patients with youth-onset T2D and reversed by SGLT2i treatment into the HumanBase functional network. Community clustering of the network was used to identify tightly connected sets of genes using the HumanBase module detection function.[23] We also conducted canonical pathway enrichment, upstream regulator, and

Table 1 | Baseline characteristics of the total and placebo and canagliflozin-treated population

Characteristic	Total ($n = 3521$)	Placebo ($n = 1181$)	Canagliflozin ($n = 2340$)
Age, yr	62.8 ($\pm$7.8)	62.6 ($\pm$7.8)	62.9 ($\pm$7.8)
Male sex	2352 (66.8)	790 (66.9)	1562 (66.8)
History of heart failure	471 (13.4)	173 (14.7)	298 (12.7)
Duration of diabetes, yr	13.6 ($\pm$7.5)	13.3 ($\pm$7.5)	13.7 ($\pm$7.5)
History of CV disease	2087 (59.3)	698 (59.1)	1389 (59.4)
BMI, kg/m^2	32.7 ($\pm$6.1)	32.6 ($\pm$6.2)	32.7 ($\pm$6.1)
Systolic BP, mm Hg	136.7 ($\pm$15.8)	137.2 ($\pm$15.8)	136.4 ($\pm$15.9)
Diastolic BP, mm Hg	77.6 ($\pm$9.8)	78.1 ($\pm$9.8)	77.3 ($\pm$9.7)
HbA1c			
mmol/mol	65.8 ($\pm$10.0)	65.7 ($\pm$9.9)	65.9 ($\pm$10.0)
%	8.2 ($\pm$0.9)	8.2 ($\pm$0.9)	8.2 ($\pm$0.9)
LDL, mmol/ml	2.3 ($\pm$0.9)	2.3 ($\pm$0.9)	2.3 ($\pm$0.9)
HDL, mmol/ml	1.2 ($\pm$0.3)	1.2 ($\pm$0.3)	1.2 ($\pm$0.3)
eGFR, ml/min per 1.73 m^2	77.0 ($\pm$18.7)	76.9 ($\pm$18.8)	77.0 ($\pm$18.7)
<60	576 (16.4)	203 (17.2)	373 (15.9)
≥60	2945 (83.6)	978 (82.8)	1967 (84.1)
UACR, mg/g	11.6 (6.4, 35.1)	11.5 (6.3, 37.0)	11.6 (6.5, 34.4)
Normoalbuminuria	2545 (72.3)	843 (71.4)	1702 (72.7)
Microalbuminuria	776 (22.0)	257 (21.8)	519 (22.2)
Macroalbuminuria	200 (5.7)	81 (6.9)	119 (5.1)
uEGF, pg/ml	4570 (2608, 7777)	4560 (2632, 7847)	4570 (2594, 7754)
uEGF/Cr, ng/mg	5.1 (3.4, 7.8)	5.2 (3.5, 7.6)	5.1 (3.3, 7.9)

Cr, creatinine; CV, cardiovascular; BMI, body mass index; BP, blood pressure; eGFR, estimated glomerular filtration rate; HbA1c, hemoglobin A1c; HDL, high-density lipoprotein; IQR, interquartile range; LDL, low-density lipoprotein; UACR, urinary albumin-to-creatinine ratio; uEGF, urinary epidermal growth factor.
Continuous variables are reported as mean ($\pm$ SD), or median IQR. Categorical variables are reported as quantity (percentage).

network analysis using Ingenuity Pathway Analysis (IPA, Qiagen) and presented the graphical summary of these analytical results.

Results were deemed significant when $P < 0.05$, except when otherwise stated. All analyses were performed in SAS version 9.4 (SAS Institute) and Stata version 16.1 (StataCorp).

RESULTS
CANVAS study population
Of the 4330 included participants in the CANVAS trial, 3521 (81.3%) had available urine samples to be used to measure uEGF and determine uEGF/Cr at baseline, and 2707 (76.9%) had samples both at baseline and at 52 weeks of follow-up (Supplementary Figure S1). Of the 2707 participants, 15 were excluded from the analysis of the association of 1-year change in uEGF/Cr with the composite kidney outcome, as these participants experienced the composite kidney outcome during the first year of follow-up. Baseline characteristics of the 3521 participants are shown in Table 1. The characteristics of the groups allocated to treatment with canagliflozin, compared to placebo, were well balanced and were similar to the baseline characteristics for the overall CANVAS trial population reported previously. The mean uEGF and uEGR/Cr at baseline in the combined canagliflozin and placebo groups were 4570 pg/ml and 5.1 ng/mg, respectively. Baseline characteristics in quartiles of baseline uEGF/Cr are presented in Supplementary Table S1.

Association of uEGF/Cr with the composite kidney outcome
The median follow-up duration of the 3521 participants was 6.1 years (interquartile range 5.8, 6.4), during which 134 participants experienced the composite kidney outcome. In general, the Pearson correlations between uEGF/Cr and other covariates were modest to weak (Supplementary Figure S2). In longitudinal analyses, baseline uEGF/Cr was found to be significantly associated with the composite kidney outcome, with a corresponding HR per doubling of uEGF/Cr in the fully adjusted model of 0.88 (95% confidence interval [CI] 0.78, 0.99; $P = 0.04$; Table 2). Categorical assessment of the association between uEGF/Cr and the composite kidney outcome revealed that participants in the 2 upper quartiles of the uEGF/Cr distribution had a statistically significant 2-fold lower risk for the composite kidney outcome, compared to that in the first quartile (Table 2). Further assessments of the association in subgroups defined by baseline patient characteristics showed no significant difference across these subgroups (Figure 1).

Effect of canagliflozin on the composite kidney outcome by baseline uEGF/Cr level
Compared to placebo, canagliflozin reduced the composite kidney outcome in the overall population by 41% (HR 0.59; 95% CI 0.42, 0.83; $P < 0.002$). Fitting uEGF/Cr as a continuous and as a categorical variable showed no evidence that the effect of canagliflozin on the composite kidney outcome varied by baseline uEGF/Cr level (both P values for heterogeneity > 0.20; Figure 2).

Effect of canagliflozin on uEGF/Cr
Overall, compared to placebo, the mean increase with canagliflozin was 7.3% (95% CI 2.0, 12.8; $P = 0.01$). This effect of canagliflozin was consistent in key patient subgroups (Table 3).

Association of the 1-year change in uEGF/Cr with the composite kidney outcome
The median baseline uEGF/Cr of the 2707 participants with available uEGF/Cr at baseline and week 52 was 5.25 ng/mg.

Table 2 | Associations of baseline uEGF/Cr with the composite kidney outcome (40% eGFR decline/kidney failure/renal death)

uEGF/Cr	Model 1		Model 2		Model 3		Model 4	
	HR (95% CI)	P	HR (95% CI)	P	HR (95% CI)	P	HR (95% CI)	P
Quartile 1	(Reference)		(Reference)		(Reference)		(Reference)	
Quartile 2	0.7 (0.4, 1.0)	0.07	0.7 (0.5, 1.1)	0.10	0.7 (0.5, 1.1)	0.11	0.8 (0.6, 1.3)	0.46
Quartile 3	0.4 (0.2, 0.6)	<0.01	0.4 (0.2, 0.6)	<0.01	0.4 (0.2, 0.7)	<0.01	0.5 (0.3, 0.8)	0.01
Quartile 4	0.3 (0.2, 0.6)	<0.01	0.4 (0.2, 0.6)	<0.01	0.4 (0.2, 0.6)	<0.01	0.5 (0.3, 0.9)	0.03
Per doubling	0.8 (0.8, 0.9)	<0.01	0.8 (0.8, 0.9)	<0.01	0.9 (0.8, 0.9)	<0.01	0.9 (0.8, 1.0)	0.04

CI, confidence interval; eGFR, estimated glomerular filtration rate; HbA1c, hemoglobin A1c; HR, hazard ratio; uEGF/Cr, urinary epidermal growth factor to creatinine ratio.
The table presents analyses of the association between uEGF/Cr with the composite kidney outcome when uEGF/Cr is modeled as a categorical (quartiles) and as a continuous (per doubling) variable.
Models are adjusted for the following covariates: model 1—age, sex, race, and randomized treatment; model 2—covariates of model 1 + HbA1c, systolic blood pressure, body mass index, low-density lipoprotein, high-density lipoprotein, and history of cardiovascular disease; model 3—covariates of model 2 + baseline estimated glomerular filtration rate; model 4—covariates of model 3 + log-transformed baseline urinary albumin-to-creatinine ratio.

Among these participants, 110 (4.1%) experienced the composite kidney outcome after 1 year of randomization. Covariates used in multivariable Cox proportional analysis, in general, were correlated weakly with the change in uEGF/Cr, except for baseline uEGF/Cr (Supplementary Figure S3). When adjusted for all covariates, each doubling of uEGF/Cr from baseline to year 1 was significantly associated with a decreased risk of subsequent kidney outcomes, with a corresponding HR of 0.79 (95% CI 0.72, 0.85; P < 0.01; Table 4). When uGFR/Cr was categorized in quartiles, the 2 upper quartiles, in which participants had an increase in uEGF/Cr, exhibited a 2-fold lower risk of experiencing the composite kidney outcome, compared to the second quartile, which had a modest decrease in mean uEGF/Cr from baseline (Table 4). The change in uEGF/Cr at year 1 was independently associated with the composite kidney outcome in both the canagliflozin and placebo groups (Supplementary Table S2).

Exploration of the molecular mechanism underlying uEGF/Cr association with improved kidney outcome after SGLT2i treatment

To explore the molecular mechanisms underlying the association of uEGF/Cr with improved kidney outcome in patients treated with the SGLT2i, we investigated the *EGF* mRNA levels following SGLT2 inhibition at the single-cell kidney tissue level in research biopsies in young persons with T2D at high risk of diabetic kidney disease. Healthy young persons were also included as a separate group. The baseline characteristics of participants were published previously.[14] Analysis of the scRNA-seq data from 22 participants

Composite kidney outcome

Subgroup	Events/patients		HR (95% CI)	*P* for heterogeneity
uEGF/Cr				
Overall	134/3521		0.88 (0.78, 0.99)	
Treatment				0.87
Placebo	60/1181		0.86 (0.74, 1.01)	
Canagliflozin	74/2340		0.88 (0.73, 1.05)	
Age				0.74
<65 yr	75/2068		0.90 (0.77, 1.06)	
≥65 yr	59/1453		0.81 (0.63, 1.03)	
Sex				0.30
Male	96/2352		0.92 (0.79, 1.07)	
Female	38/1169		0.69 (0.53, 0.91)	
UACR				0.46
<30 mg/g	50/2545		0.88 (0.73, 1.06)	
≥30 mg/g	84/976		0.89 (0.74, 1.06)	
eGFR				0.38
<60 ml/min per 1.73 m²	35/576		0.79 (0.59, 1.06)	
≥60 ml/min per 1.73 m²	99/2945		0.90 (0.77, 1.05)	
CV disease history				0.46
No	37/1434		0.86 (0.71, 1.04)	
Yes	97/2087		0.90 (0.77, 1.05)	

0.5　　1.0　　2.0
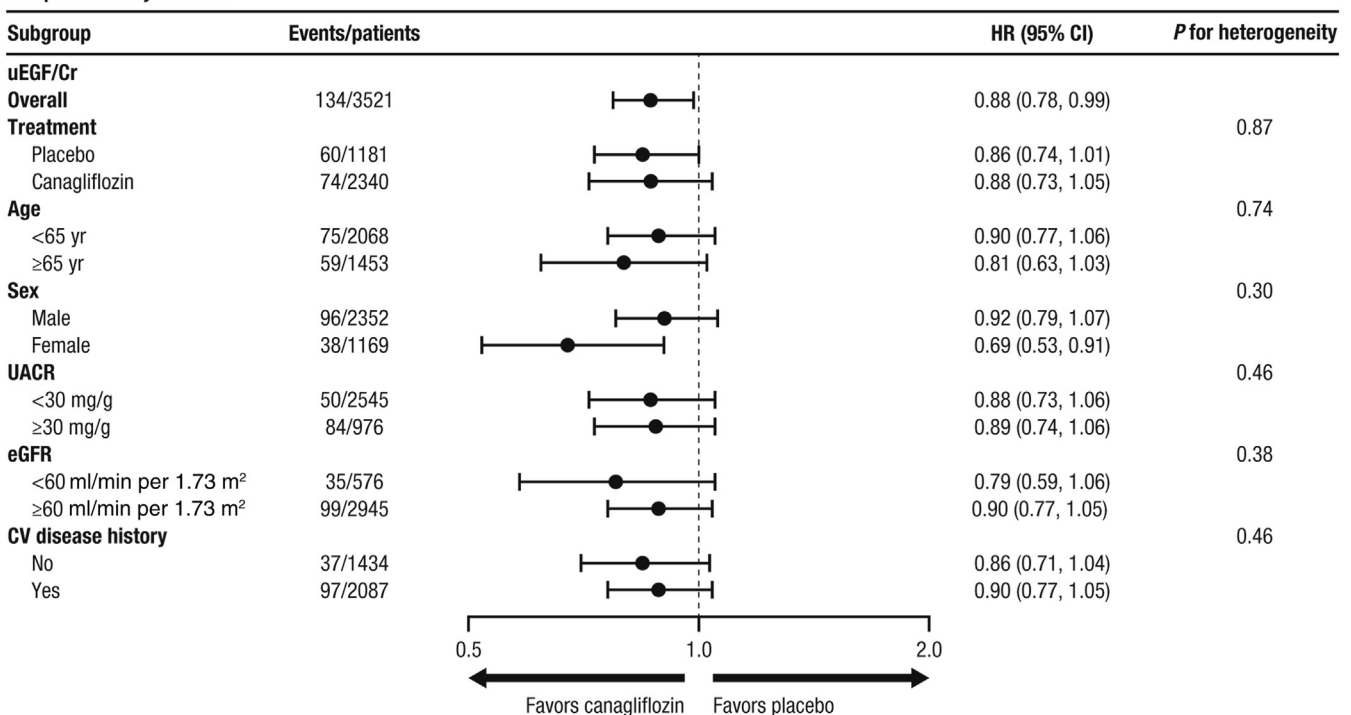← Favors canagliflozin　Favors placebo →

Figure 1 | Associations of baseline urinary epidermal growth factor-to-creatinine ratio (uEGF/Cr) with the composite kidney outcome by subpopulations defined by treatment allocation, age, sex, urinary albumin-to-creatinine ratio (UACR), estimated glomerular filtration rate (eGFR), and cardiovascular (CV) disease history. Hazard ratios (HRs) are expressed per doubling of uEGF/Cr. CI, confidence interval.

Composite kidney outcome

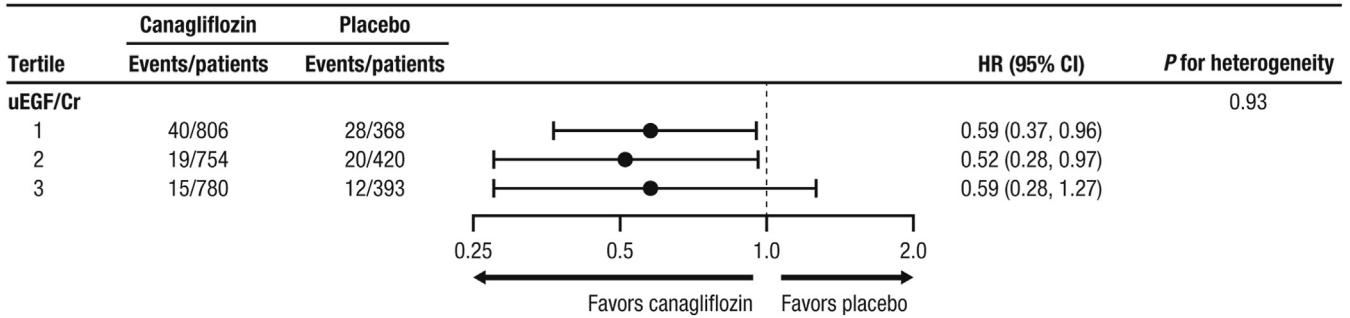| Tertile	Canagliflozin Events/patients	Placebo Events/patients		HR (95% CI)	P for heterogeneity
uEGF/Cr					0.93
1	40/806	28/368		0.59 (0.37, 0.96)	
2	19/754	20/420		0.52 (0.28, 0.97)	
3	15/780	12/393		0.59 (0.28, 1.27)	

Figure 2 | Forest plot of the unadjusted effect of canagliflozin on the composite kidney outcome by tertiles of baseline urinary epidermal growth factor-to-creatinine ratio (uEGF/Cr). *P*-heteroegeneity for uEGF/Cr when modeled as a continuous variable was 0.20. CI, confidence interval; HR, hazard ratio.

resulted in 50,601 cells that could be grouped into 18 cell clusters (Figure 3a; Supplementary Figure S4A) representing the entire spectrum of kidney cell types along the nephron as well as tissue-resident immune cells, and each cell cluster had a robust representation of the 3 biopsy groups (Supplementary Figure S4B).[14]

EGF was expressed abundantly in the TAL and the DCT cell clusters with sporadic expression in the ascending thin loop of Henle cell cluster (Figure 3b) across 3 groups, as follows: healthy controls (HCs; *n* = 6); 10 participants with T2D who had been prescribed SGLT2i [T2Di(+)] (*n* = 10); and 6 who had not been prescribed SGLT2i [T2Di(–)]. Consistent with previous reports, *EGF* was colocalized with the TAL-specific marker uromodulin (*UMOD*) in TAL cells, and with DCT-specific marker gene solute carrier family 12 member 3 (*SLC12A3*) in DCT cells (Supplementary Figure S5).[7,24–28]

To examine the influence of SGLT2i on intra-kidney *EGF* expression and its downstream gene network, additional analyses focused on the TAL cells representing the largest cell cluster that expresses *EGF* transcripts. As demonstrated in dot plot analyses, the mean expression of EGF mRNA in the TAL of participants not using SGLT2i, T2Di(–) was significantly lower, compared to that in reference tissues from HCs (age-adjusted *P* value = 1.94E–60; Supplementary Table S3; Figure 3c). In contrast, in T2Di(+) participants, we observed a higher EGF mRNA expression level (age-adjusted *P* value=

0.002; Supplementary Table S3; Figure 3c). The percentage of TAL cells expressing EGF (~90%) was not different between HCs and young persons with T2D who were using versus who were not using SGLT2i.

Potential impact of SGLT2i on EGF-coexpressing functional gene networks

Genes that were differentially expressed between TAL cells with EGF expression (EGF+; about 90% of the TAL cells) versus those without detectable EGF transcripts (EGF–; approximately 10% of the TAL cells) were mapped to their cellular functional context (Figure 4). EGF positivity was defined as a normalized expression value of EGF greater than zero (EGF > 0).

In young persons with T2D using SGLT2i treatment, we identified 459 genes that were differentially expressed in EGF+ versus EGF– TAL cells, with an adjusted *P* value < 1e^{-20} and a fold change > 1.20 or < 0.83. Of these, 412 genes (89.8%) had higher expression in EGF+ TAL cells, compared to that in the EGF– TAL cells. *UMOD*, *MALAT1*, *XIST*, *CLDN10*, *CXCL12*, *DDX17*, *SLC12A1*, *NEAT1*, *KNG1*, and *HSP90B1* were the top 10 genes among these highly expressed genes in EGF+ TAL cells. In young persons with T2D who were not using SGLT2i, only 183 genes were significantly differentially expressed in EGF+ versus EGF– TAL cells, based on the same statistical and fold-change cutoffs (Supplementary Table S4).

Table 3 | Effect of 52 weeks of treatment with canagliflozin, compared to placebo, on uEGF/Cr

	Geometric mean baseline uEGF/Cr, ng/mg		Change from baseline at week 52, %		Between-group difference, % (95% CI)	P[a]	P for interaction
	Canagliflozin	Placebo	Canagliflozin (95% CI)	Placebo (95% CI)			
Overall	5.10	5.25	–1.4 (–4.2, 1.4)	–8.1 (–11.8, –4.2)	7.3 (2.0, 12.8)	0.01	
UACR							0.73
<30	5.45	5.45	–1.4 (–4.8, 2.1)	–8.6 (–13.1, –3.9)	7.9 (1.5, 14.7)	0.02	
≥30	4.26	4.75	–1.5 (–6.1, 3.4)	–6.3 (–12.8, –0.6)	5.2 (–3.5, 14.6)	0.25	
eGFR							0.57
<60	3.21	3.96	–4.6 (–13.4, 5.1)	–8.8 (–20.8, 5.1)	4.6 (–12.0, 24.2)	0.61	
≥60	5.52	5.52	–0.8 (–3.6, 2.0)	–8.0 (–11.8, –4.1)	7.8 (2.5, 13.4)	<0.01	

CI, confidence interval; eGFR, estimated glomerular filtration rate; UACR, urinary albumin-to-creatinine ratio; uEGF/Cr, urinary epidermal growth factor to creatinine ratio.
[a]*P* value indicates the between-group difference in uEGF.
Data are presented in the overall population and in subgroups defined by baseline UACR, and eGFR.

Table 4 | Associations of the change in uEGF from baseline to year 1 with the composite kidney outcome (40% eGFR decline/kidney failure/renal death)

uEGF/Cr	Median change, %	Model 1 HR (95% CI)	P	Model 2 HR (95% CI)	P	Model 3 HR (95% CI)	P	Model 4 HR (95% CI)	P	Model 5 HR (95% CI)	P
Quartile 1	−53.3	1.3 (0.9, 2.1)	0.21	1.2 (0.8, 1.9)	0.40	1.3 (0.8, 2.0)	0.26	1.3 (0.9, 2.1)	0.20	1.3 (0.8, 2.1)	0.22
Quartile 2	−12.9	Reference		Reference		Reference		Reference		Reference	
Quartile 3	8.4	0.3 (0.2, 0.6)	<0.01	0.4 (0.2, 0.7)	<0.01	0.4 (0.2, 0.7)	<0.01	0.4 (0.2, 0.8)	0.01	0.4 (0.2, 0.8)	0.01
Quartile 4	41.5	0.3 (0.2, 0.6)	<0.01	0.4 (0.2, 0.8)	0.01	0.4 (0.2, 0.7)	<0.01	0.5 (0.2, 0.9)	0.02	0.4 (0.2, 0.8)	0.01
Per doubling		0.8 (0.7, 0.9)	<0.01	0.8 (0.7, 0.9)	<0.01	0.8 (0.7, 0.9)	<0.01	0.8 (0.7, 0.9)	<0.01	0.8 (0.7, 0.9)	<0.01

CI, confidence interval; CV, cardiovascular; eGFR, estimated glomerular filtration rate; HbA1c, hemoglobin A1c; HDL, high-density lipoprotein; HR, hazard ratio; LDL, low-density lipoprotein; UACR, urinary albumin-to-creatinine ratio; uEGF, urinary epidermal growth factor; uEGF/Cr, urinary epidermal growth factor to creatinine ratio.
uEGF/Cr change from baseline was stratified in quartiles of change and analyzed as a categorical variable as well as a continuous variables with HRs expressed per doubling of uEGF from baseline to week 52.
Models are adjusted for the following covariates: model 1—baseline uEGF, age, sex, race, and randomized treatment; model 2—covariates of model 1 + change in eGFR from baseline to year 1 and baseline eGFR; model 3—covariates of model 1 + change in UACR from baseline to year 1 and baseline UACR; model 4—covariates of model 1 + change in eGFR and UACR from baseline to year 1 and baseline eGFR and UACR; model 5—covariates of model 1 + history of CV disease, HbA1c, systolic blood pressure, body mass index, LDL, HDL, eGFR, baseline UACR and change in eGFR, UACR, systolic blood pressure, body mass index, and HbA1c from baseline to year 1.
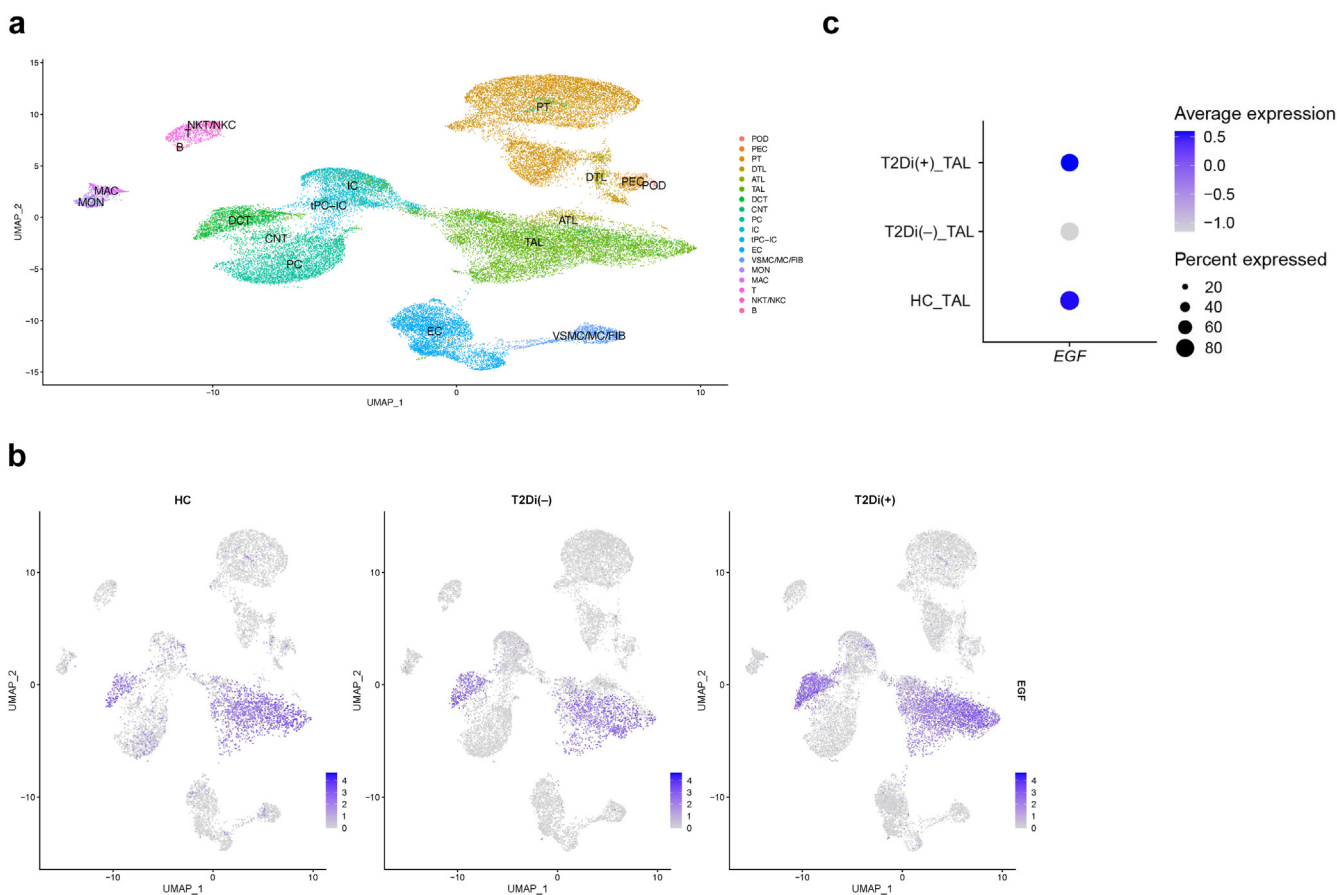
Figure 3 | Single-cell RNA sequencing (ScRNA-seq) analysis showing restricted expression of epidermal growth factor (EGF) mRNA in thick ascending loop of Henle (TAL) and distal convoluted tubule (DCT) cells. (a) Unsupervised clustering of cells from reference tissue from healthy controls (HC) and patients with type 2 diabetes (T2D) with (i+) and without (i−) sodium–glucose cotransporter 2 inhibitor (SGLT2i) treatment. (b) For all groups [HC; T2Di(−) and T2Di(+)], EGF mRNA expressing cells (blue dots) were limited to the TAL and DCT clusters. (c) Dot plots analysis of EGF expression in TAL cell cluster from kidney biopsies of healthy participants (HC_TAL), young persons with T2D [T2Di (−)_TAL], and young persons with T2D treated with SGLT2i [T2Di(+)_TAL]. Size of dots reflecting fraction of cells (%) expressing EGF mRNA, and color intensity indicating mean expression levels. The EGF expression is lowest in T2Di (−), with significantly higher expression in HC [age adjusted $P = 1.94E-60$, compared to T2Di(−)] and T2Di(+) [age-adjusted $P = 0.002$, compared to T2Di(−)] groups. ATL, ascending thin loop of Henle; B, B cells; CNT, connecting tubule; DKD, diabetic kidney disease; DTL, descending loop of Henle; EC, endothelial cell; FIB, fibroblast; IC, intercalated cell; IC-A, intercalated cell-type A; MAC, macrophage; MC, mesangial cell; MON, monocyte; NKT, natural killer T; NKC, natural killer cell; PC, principal cell; PEC, parietal epithelial cell; POD, podocyte; PT, proximal tubular epithelial cell; T, T cell; tPC-IC, transitional principal and intercalated cell; UMAP, uniform manifold approximation and projection; VSMC, vascular smooth muscle cell.
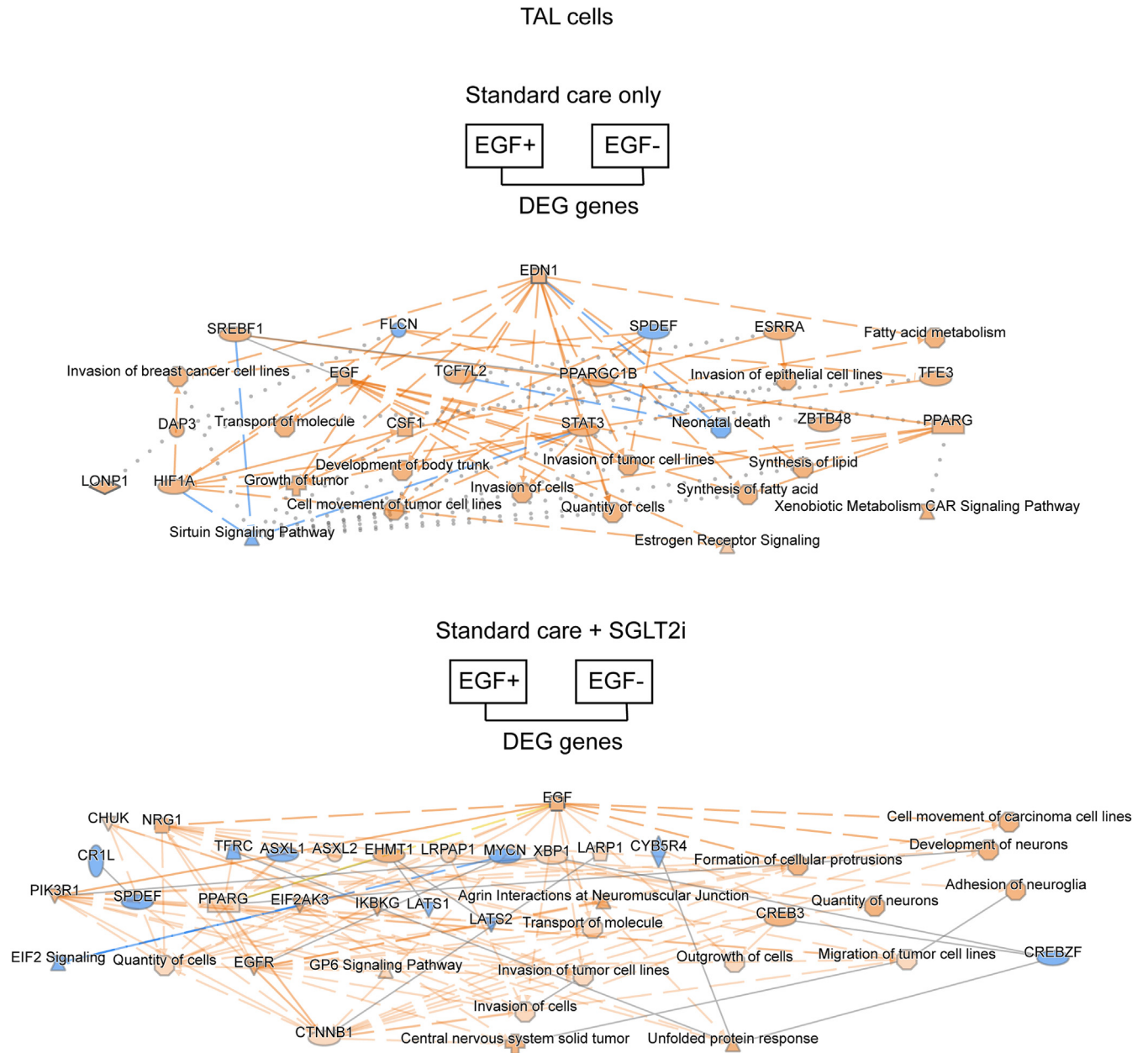
Figure 4 | Hierarchical summary of significantly enriched pathways/networks and upstream regulators (cytokines, growth factors and transcriptional factors) in epidermal growth factor (EGF) coexpressing gene signatures in thick ascending loops of Henle (TALs) of patients with/without sodium–glucose cotransporter 2 inhibitor (SGLT2i) treatment. Endothelin 1 (EDN1) as the top node of the EGF coregulated gene signature in TAL cells of diabetic kidney disease (DKD) patients without an SGLT2i (upper panel), whereas in patients treated with an SGLT2i, EGF is the top node impacting enriched pathways/networks (lower panel). Light orange nodes represent upregulated/activated genes/pathways whereas light blue nodes represent down-regulated/repressed genes/pathways. Light orange and blue lines indicate leading to activation or inhibition, respectively. Dotted gray lines indicate inferred relationship. Disconnected lines indicate indirect relationship. Gray lines indicate direct relationship. ASXL1, additional sex combs like transcriptional regulator 1; ASXL2, additional sex combs like transcriptional regulator 2; CAR, calcium sensing receptor; CHUK, conserved helix-loop-helix ubiquitous kinase; CREB3, cAMP responsive element binding protein 3; CR1L, complement component (3b/4b) receptor 1-like; CSF1, colony stimulating factor 1; CYB5R4, cytochrome b5 reductase 4; EGF+, epidermal growth factor expressing; EGF−, epidermal growth factor non-expressing; EHMT1, euchromatic histone-lysine N-methyltransferase 1; EIF2, eukaryotic initiation factor 2; EIF2AK3, eukaryotic translation initiation factor 2-alpha kinase 3; ESRRA, estrogen-related receptor alpha; DAP3, death associated protein 3; DEG, differentially expressed gene; FDR, false discovery rate; GP6, glycoprotein VI; HIF1A, hypoxia inducible factor 1, alpha subunit; Ilog2FCI, absolute value of Log2 transformed fold change; LARP1, La ribonucleoprotein 1; LATS1, large tumor suppressor kinase 1; LATS2, large tumor suppressor kinase 2; LONP1, lon peptidase 1; LRPAP1, low density lipoprotein receptor-related protein associated protein 1; MYCN, v-myc avian myelocytomatosis viral oncogene neuroblastoma derived homolog; NRG1, neuregulin 1; PPARG, peroxisome proliferator-activated receptor gamma; PPARGC1B, peroxisome proliferator-activated receptor gamma, coactivator 1 beta; PIK3R1, phosphoinositide-3-kinase, regulatory subunit 1; SPDEF, SAM pointed domain containing ETS transcription factor; SREBF1, sterol regulatory element binding transcription factor 1; STAT3, signal transducer and activator of transcription 3; TCF7L2, transcription factor 7-like 2; TFE3, transcription factor binding to IGHM enhancer 3; TFRC, transferrin receptor; XBP1, X-box binding protein 1; ZBTB48, zinc finger and BTB domain containing 48.

To unravel the effect of SGLT2i on the above functional gene networks in these 2 gene sets, we compared enriched molecular pathways in patients under standard care alone versus in those treated with SGLT2i as well. We used ingenuity pathway analysis to reveal the enriched canonical pathways, gene networks, and upstream regulators (cytokines, growth factors, and transcriptional factors) in these 2 gene sets. The hierarchical graphical summary (Figure 4) demonstrates that endothelin-1 is the key regulator modulating gene and interacting networks derived from 183 genes that are differentially expressed in *EGF+* versus *EGF–* TAL cells in T2D patients under standard care only, whereas EGF was the factor positioned at the apex of the hierarchical regulatory cascade in T2D patients treated with an SGLT2i. We also performed a similar analysis on HC cells, but only 12 genes met the same cutoff criteria, making it difficult to perform a reliable enrichment analysis. To increase the number of genes for analysis, we relaxed the selection criteria to include genes with an adjusted *P* value < 0.05 and a fold-change > 1.20 or < 0.83, resulting in the identification of 244 genes. Pathway analysis of these 244 genes showed that EGF receptor was the top node of the hierarchical regulation cascade in healthy individuals (Supplementary Figure S6).

DISCUSSION

The precise mechanism by which SGLT2i provide kidney protection is incompletely understood. By using cell type–specific gene expression analysis of T2D research biopsies, coupled with a large repository of a randomized controlled trial, we demonstrate that SGLT2 inhibition with canagliflozin increases *EGF* mRNA in distal tubular epithelial cells, with a shift toward the gene-regulation network toward differentiated tubular function from an endothelin-1–centered regulatory network. The impact of canagliflozin on EGF regulation appears to be clinically important; in our large cohort of patients with T2D, canagliflozin increased uEGF, an effect that is correlated tightly with intra-kidney EGF transcript levels.[7] Further, both basal and early changes in uEGF during canagliflozin treatment were associated with subsequent kidney outcomes. Collectively, these data suggest that EGF may contribute to the kidney-protective effect of canagliflozin and may be used clinically as a pharmacodynamic response marker.

As a noninvasive biomarker for kidney distal tubular cell integrity, uEGF level is highly positively correlated with tubulointerstitial *EGF* mRNA levels, and lower levels of both are associated with higher levels of interstitial fibrosis and tubular atrophy.[7] EGF enhances kidney tubular cell regeneration and repair and accelerates the recovery of kidney function in multiple rodent models of kidney injury, establishing its important protective role in kidney tubular cell function.[29–35] In the current study, a significantly reduced level of *EGF* mRNA was observed in TAL cells of young persons with T2D using standard of care, compared to that of reference tissue from healthy participants, suggesting an impaired capacity for repair of TAL cells. Our previous work suggested that EGF may function as a master

regulator in distal tubular cells by modulating the downstream target genes, many of which play an important role in kidney repair and are correlated with kidney function change (eGFR slope) in patients with CKD.[7] With EGF levels consistently repressed in diabetic kidney disease,[7,9,36,37] a dysregulation of the EGF downstream signaling cascade in diabetic conditions might be one factor contributing to the decreased kidney repair capacity seen in patients with diabetic kidney disease.

SGLT2i may at least partially reverse this pathogenic process by promoting EGF expression. In our single-cell kidney biopsy studies, the *EGF* mRNA level was significantly higher in patients treated with SGLT2i, compared to that in an untreated control group, and similar to that of HCs. This finding suggests that treatment with SGLT2i may influence the downstream EGF signalling cascade, which mediates repair and improves TAL homeostasis. Our findings at the single-cell level support the uEGF biomarker results from the CANVAS study demonstrating that, in a large cohort of patients with T2D, the uEGF level decreased during placebo treatment, whereas this effect was attenuated with canagliflozin treatment.

How inhibition of SGLT2 transporters, which are expressed only in proximal tubular cells, translates to improved distal tubular cell homeostasis is incompletely understood. In a recent study, we demonstrated that a decreased level of *SLC5A2* mRNA expression in T2Di(+) across all proximal tubule subclusters, led by SGLT2i, is associated with metabolic reprogramming and reestablished the transcriptional programs of physiological renal energetics across the nephron (gene lists are available in Schaub *et al.* in Supplementary Table 2, https://www.jci.org/articles/view/164486/sd/2), with a particularly prominent effect on TAL.[15] To further define the impact of SGLT2i, *EGF* co-regulated gene networks were explored at the single-cell transcriptome level in key cells that express *EGF*, such as TAL cell cluster, of patients using versus not using canagliflozin. We observed a close to 1.5-fold increase in the number of genes co-regulated with EGF in patients treated with SGLT2i, compared to those without such treatment (459 vs. 183 genes), indicating a reestablished *EGF* coexpression program in TAL with canagliflozin. This unbiased, data-driven approach revealed the activation of the endothelin-1 pathway as a key mediator associated with *EGF+* TAL cells in T2D. Endothelin activation is known to be triggered by a wide range of stimuli that are associated with diabetic kidney disease, including but not limited to hypoxia,[38] reactive oxygen species,[39] and hyperglycemia.[40–42] Endothelin-1 is therefore considered a proinflammatory and profibrotic factor.[43] A similar analysis, conducted for the EGF receptor coexpression program in tubular cells, supported the robust presence of EGF as a top regulator in SGLT2i-treated patients but not in untreated patients, further supporting our hypothesis. In our study, canagliflozin clearly impacted the dynamics of the EGF-associated regulatory network in distal tubular cells of young persons with T2D and orchestrated the key mediators involved in kidney repair.

Our study has implications for clinical practice. In keeping with results of previous studies, our data show that a lower uEGF level can serve as an independent risk marker of CKD progression. Previous studies enrolled patients with CKD and demonstrated strong and independent associations between uEGF level and kidney disease progression. We confirm and extend these findings to patients with T2D at high cardiovascular risk. Our data also suggest that uEGF can be used clinically as a pharmacodynamic response marker, as the magnitude of uEGF increase during treatment with canagliflozin was associated with long-term kidney outcomes, independent of other risk markers of kidney function decline. Collectively, the current data support a potential future role for uEGF as a risk and pharmacodynamic response marker for canagliflozin. The question of whether targeting specific thresholds of uEGF with canagliflozin will derive more kidney protection, compared to that in patients in whom uEGF does not increase, could not be answered reliably in this study because we stratified our cohort based on a postrandomization variable. Answering this question requires a prospective clinical trial with an active run-in period to identify individuals who do and those who do not achieve an increase in uEGF/Cr with canagliflozin, and are subsequently randomized to continue canagliflozin or transition to placebo.

This study has limitations. First, because our study was a *post hoc* analysis, we cannot exclude the possibility of chance findings. Furthermore, although our statistical analyses were adjusted for various confounders, the possibility of residual confounding cannot be excluded. Nonetheless, the HRs for the association between uEGF/Cr and kidney outcomes were consistent in various models, adjusting for multiple potential confounders, supporting the robustness of our findings. Additionally, the CANVAS trial enrolled patients with T2D who were at high risk of or had established cardiovascular disease. The number of patients with CKD and the number of kidney outcomes were relatively low, which reduced statistical power and the precision of the effect estimates. Further studies are required in patients with T2D and CKD. The youth-onset T2D kidney research biopsy specimens used in this analysis were collected in an observational study. SGLT2i use was prescribed at the discretion of patients' physicians, and results could be influenced by indication bias. Different cohorts were used for the biomarker and single-cell transcriptomic analysis, owing to unavailability of the biopsy from the CANVAS study for scRNA-seq analysis. Instead, we constructed our study by assessing uEGF in urine samples collected at the time of biopsy from patients whose kidney tissue were used in the scRNA-seq analysis. The uEGF/Cr level in patients treated with SGLT2i {T2Di(+) [$n = 9$; 1 patient urine sample is missing]} showed a trend toward being higher, compared to that in those who did not receive treatment [T2Di (–); $n = 6$]. Although this difference did not reach statistical significance ($P = 0.21$), likely because of the small sample size, the emerging trend of uEGF/Cr data (not shown) supports our biomarker discovery from the CANVAS study. Additionally, a relatively small sample size was used in making the comparisons among groups in the scRNA-seq analyses. Although the sample size is small, the total cell number used for the reported analysis is adequate for reliable discovery. A proof-of-concept example was demonstrated in the primary publication, which reported that decreased levels of phosphorylated S6 protein in proximal and distal tubules were observed via immunohistochemical staining in T2Di(+) individuals. These findings confirmed changes in mammalian target of rapamycin complex 1 (mTORC1) pathway activity.[14] Although we are aware of this limitation, we focused our key analysis on cell clusters with an abundance of cells. Accordingly, the integrative analysis enabled us to utilize the advantages of both cohorts, thereby compensating for their separate limitations, and corroborating the same conclusion. The molecular data should be considered to be hypothesis-generating only, as causality cannot be implied, and call for further experimental validation. A computational approach that integrates expression data from proximal tubule and TAL cells with prior knowledge on signaling and gene regulatory networks could be used to predict ligand–target interactions.[44] This approach can be used in future studies to elucidate the intermediate steps that connect the SGLT2i-driven transcriptional program in proximal tubule with the upregulation of EGF in TAL and activation of EGF–EGF receptor signaling in the nephron, leading to kidney repair and regeneration. Finally, another point that is important to underscore is the difference in age and kidney function between the participants in the CANVAS trial and those in the kidney biopsy study.

In conclusion, SGLT2i treatment with canagliflozin is associated with increased kidney tissue expression of EGF in young persons with T2D, which in turn activated a gene-regulation network associated with EGF-associated kidney repair. In patients with T2D who are at high cardiovascular disease risk, uEGF and its changes over a 1-year time period have prognostic value for kidney outcomes. Canagliflozin increases the level of uEGF, which supports a role for uEGF as a pharmacodynamic response marker to monitor the efficacy of canagliflozin over time.

DATA STATEMENT

ACKNOWLEDGMENTS

AUTHOR CONTRIBUTIONS

TS, WJ, MK, PB, and HJLH were involved in the study design, conduct of the studies, data collection, and interpretation. TS, WJ, and HJLH wrote the first draft of the manuscript. TS and VN performed statistical analyses. WJ and VN designed and performed pathway analyses. VN, PL, RM, and EAO performed single-cell RNA sequence analyses. LP, TV, and RGN were involved in the IMPROVE and RENAL-HEIR studies and collected kidney biopsies. CA, BN, and MKH were involved in the study design and data collection of the CANVAS trial. All authors reviewed the manuscript drafts, provided approval of the final version for submission, and take responsibility for the accuracy and integrity of the data. The first 2 authors share first authorship, and the order was assigned by seniority, with junior faculty members being offered the first position. HJLH had full access to the data in the study and had final responsibility for the decision to submit for publication.

SUPPLEMENTARY MATERIAL

Supplementary File (PDF)

Supplementary Table S1. Baseline characteristics of the total population by quartiles of urinary epidermal growth factor (uEGF).
Supplementary Table S2. Associations of the change in urinary epidermal growth factor (uEGF) from baseline to year 1 with the composite kidney outcome (40% estimated glomerular filtration rate [eGFR] decline/kidney failure/renal death) separate for the placebo and canagliflozin-treated groups.
Supplementary Table S3. Comparison of *EGF* expression in thick ascending loop (TAL) clusters between three biopsy groups. Welch *t* test was used to compare the differences, and Bonferroni-adjusted *P* value was presented.
Supplementary Table S4. Genes that are co-regulated with EGF in thick ascending loop (TAL) cell clusters in biopsy groups without and with sodium glucose co-transporter 2 inhibitor (SGLT2i) treatment: type 2 diabetes (T2D)i (–) and T2Di (+).
Supplementary Figure S1. Flow diagram of available samples for measurement.
Supplementary Figure S2. Pearson correlation test of baseline urinary epidermal growth factor (uEGF)/creatinine (Cr) with covariates used in the assessment of the association of baseline uEGF/Cr with the composite kidney outcome.
Supplementary Figure S3. Pearson correlation test of the 1-year change in urinary epidermal growth factor (uEGF)/creatinine (Cr) with covariates used in the assessment of the association of the 1-year change in uEGF/Cr from baseline with the composite kidney outcome.
Supplementary Figure S4. (**A**) Uniform manifold approximation and projection (UMAP) demonstration of annotated cell clusters corresponding to major cell types in the nephron in 3 biopsy groups: healthy controls (HC; *n* = 6); type 2 diabetes without inhibitor treatment [T2Di (–); *n* = 6]; and with inhibitor [T2Di (+); *n* = 10]. (**B**) Charts displaying each cell cluster had a robust representation in the 3 biopsy groups.
Supplementary Figure S5. Co-localization of *EGF* with thick ascending loop (TAL)–specific marker gene *UMOD* and distal convoluted tubule (DCT)-specific gene *SLC12A3*.
Supplementary Figure S6. Hierarchical summary of significantly enriched pathways/networks and upstream regulators (cytokines, growth factors, and transcriptional factors) in EGF coexpressing gene signatures in thick ascending loops (TALs) of healthy controls (HCs).

REFERENCES

1. Perkovic V, Jardine MJ, Neal B, et al. Canagliflozin and renal outcomes in type 2 diabetes and nephropathy. *N Engl J Med*. 2019;380:2295–2306.
2. Neal B, Perkovic V, Mahaffey KW, et al. Canagliflozin and cardiovascular and renal events in type 2 diabetes. *N Engl J Med*. 2017;377:644–657.
3. Neuen BL, Young T, Heerspink HJL, et al. SGLT2 inhibitors for the prevention of kidney failure in patients with type 2 diabetes: a systematic review and meta-analysis. *Lancet Diabetes Endocrinol*. 2019;7: 845–854.

4. Heerspink HJL, Stefansson BV, Correa-Rotter R, et al. Dapagliflozin in patients with chronic kidney disease. *N Engl J Med*. 2020;383:1436–1446.

5. Sen T, Heerspink HJL. A kidney perspective on the mechanism of action of sodium glucose co-transporter 2 inhibitors. *Cell Metab*. 2021;33:732–739.

6. Wee P, Wang Z. Epidermal growth factor receptor cell proliferation signaling pathways. *Cancers (Basel)*. 2017;9:52.

7. Ju W, Nair V, Smith S, et al. Tissue transcriptome-driven identification of epidermal growth factor as a chronic kidney disease biomarker. *Sci Transl Med*. 2015;7:316ra193.

8. Klein J, Bascands JL, Buffin-Meyer B, Schanstra JP. Epidermal growth factor and kidney disease: a long-lasting story. *Kidney Int*. 2016;89:985–987.

9. Betz BB, Jenks SJ, Cronshaw AD, et al. Urinary peptidomics in a rodent model of diabetic nephropathy highlights epidermal growth factor as a biomarker for renal deterioration in patients with type 2 diabetes. *Kidney Int*. 2016;89:1125–1135.

10. Menon R, Otto EA, Hoover P, et al. Single cell transcriptomics identifies focal segmental glomerulosclerosis remission endothelial biomarker. *JCI Insight*. 2020;5:e133267.

11. Wu H, Malone AF, Donnelly EL, et al. Single-cell transcriptomics of a human kidney allograft biopsy specimen defines a diverse inflammatory response. *J Am Soc Nephrol*. 2018;29:2069–2080.

12. Kidney Precision Medicine Project. Protocols. Accessed July 29, 2021. https://www.kpmp.org/for-researchers#protocols

13. Otto E. Single cell RNA sequencing (scRNA-seq). Accessed July 29, 2021. https://www.protocols.io/view/single-cell-rna-sequencing- scrna-seq-7 dthi6n

14. Schaub JA, AlAkwaa FM, McCown PJ, et al. SGLT2 inhibitors mitigate kidney tubular metabolic and mTORC1 perturbations in youth-onset type 2 diabetes. *J Clin Invest*. 2023;133:e164486.

15. Liu J, Nair V, Zhao Y, et al. Multi-scalar data integration links glomerular angiopoietin-tie signaling pathway activation with progression of diabetic kidney disease. *Diabetes*. 2022;71:2664–2676.

16. Menon R, Otto EA, Sealfon R, et al. SARS-CoV-2 receptor networks in diabetic and COVID-19-associated kidney disease. *Kidney Int*. 2020;98:1502–1518.

17. Harder JL, Menon R, Otto EA, et al. Organoid single cell profiling identifies a transcriptional signature of glomerular disease. *JCI Insight*. 2019;4:e122697.

18. Menon R, Otto EA, Kokoruda A, et al. Single-cell analysis of progenitor cell dynamics and lineage specification in the human fetal kidney. *Development*. 2018;145:dev164038.

19. Arazi A, Rao DA, Berthier CC, et al. The immune cell landscape in kidneys of patients with lupus nephritis. *Nat Immunol*. 2019;20:902–914.

20. Young MD, Behjati S. SoupX removes ambient RNA contamination from droplet-based single-cell RNA sequencing data. *Gigascience*. 2020;9:giaa151.

21. Lake BB, Menon R, Winfree S, et al. An atlas of healthy and injured cell states and niches in the human kidney. *Nature*. 2023;619:585–594.

22. Menez S, Ju W, Menon R, et al. Urinary EGF and MCP-1 and risk of CKD after cardiac surgery. *JCI Insight*. 2021;6:e147464.

23. Krishnan A, Zhang R, Yao V, et al. Genome-wide prediction and functional characterization of the genetic basis of autism spectrum disorder. *Nat Neurosci*. 2016;19:1454–1462.

24. Salido EC, Lakshmanan J, Fisher DA, et al. Expression of epidermal growth factor in the rat kidney. An immunocytochemical and in situ hybridization study. *Histochemistry*. 1991;96:65–72.

25. Lev-Ran A, Hwang DL, Ben-Ezra J, Williams LE. Origin of urinary epidermal growth factor in humans: excretion of endogenous EGF and infused [131I]-human EGF and kidney histochemistry. *Clin Exp Pharmacol Physiol*. 1992;19:667–673.

26. Stein-Oakley AN, Tzanidis A, Fuller PJ, et al. Expression and distribution of epidermal growth factor in acute and chronic renal allograft rejection. *Kidney Int*. 1994;46:1207–1215.

27. Gesualdo L, Di Paolo S, Calabro A, et al. Expression of epidermal growth factor and its receptor in normal and diseased human kidney: an immunohistochemical and in situ hybridization study. *Kidney Int*. 1996;49:656–665.

28. Norvik JV, Harskamp LR, Nair V, et al. Urinary excretion of epidermal growth factor and rapid loss of kidney function. *Nephrol Dial Transplant*. 2021;36:1882–1892.

29. Humes HD, Cieslinski DA, Coimbra TM, et al. Epidermal growth factor enhances renal tubule cell regeneration and repair and accelerates the recovery of renal function in postischemic acute renal failure. *J Clin Invest*. 1989;84:1757–1761.

30. Coimbra TM, Cieslinski DA, Humes HD. Epidermal growth factor accelerates renal repair in mercuric chloride nephrotoxicity. *Am J Physiol*. 1990;259:438.

31. Norman J, Tsau YK, Bacay A, Fine LG. Epidermal growth factor accelerates functional recovery from ischaemic acute tubular necrosis in the rat: role of the epidermal growth factor receptor. *Clin Sci (Lond)*. 1990;78:445–450.

32. Morin NJ, Laurent G, Nonclercq D, et al. Epidermal growth factor accelerates renal tissue repair in a model of gentamicin nephrotoxicity in rats. *Am J Physiol*. 1992;263:806.

33. Schaudies RP, Nonclercq D, Nelson L, et al. Endogenous EGF as a potential renotrophic factor in ischemia-induced acute renal failure. *Am J Physiol*. 1993;265:425.

34. Pavlov TS, Levchenko V, O'Connor PM, et al. Deficiency of renal cortical EGF increases ENaC activity and contributes to salt-sensitive hypertension. *J Am Soc Nephrol*. 2013;24:1053–1062.

35. Yen T, Alison MR, Goodlad RA, et al. Epidermal growth factor attenuates tubular necrosis following mercuric chloride damage by regeneration of indigenous, not bone marrow-derived cells. *J Cell Mol Med*. 2015;19:463–473.

36. Wu L, Li XQ, Chang DY, et al. Associations of urinary epidermal growth factor and monocyte chemotactic protein-1 with kidney involvement in patients with diabetic kidney disease. *Nephrol Dial Transplant*. 2020;35:291–297.

37. Nowak N, Skupien J, Smiles AM, et al. Markers of early progressive renal decline in type 2 diabetes suggest different implications for etiological studies and prognostic tests development. *Kidney Int*. 2018;93:1198–1206.

38. Minchenko DO, Tsymbal DO, Riabovol OO, et al. Hypoxic regulation of EDN1, EDNRA, EDNRB, and ECE1 gene expressions in ERN1 knockdown U87 glioma cells. *Endocr Regul*. 2019;53:250–262.

39. Chen HC, Guh JY, Shin SJ, et al. Reactive oxygen species enhances endothelin-1 production of diabetic rat glomeruli in vitro and in vivo. *J Lab Clin Med*. 2000;135:309–315.

40. Hargrove GM, Dufresne J, Whiteside C, et al. Diabetes mellitus increases endothelin-1 gene transcription in rat kidney. *Kidney Int*. 2000;58:1534–1545.

41. Yamauchi T, Ohnaka K, Takayanagi R, et al. Enhanced secretion of endothelin-1 by elevated glucose levels from cultured bovine aortic endothelial cells. *FEBS Lett*. 1990;267:16–18.

42. Hattori Y, Kasai K, Nakamura T, et al. Effect of glucose and insulin on immunoreactive endothelin-1 release from cultured porcine aortic endothelial cells. *Metabolism*. 1991;40:165–169.

43. Dhaun N, Goddard J, Webb DJ. The endothelin system and its antagonism in chronic kidney disease. *J Am Soc Nephrol*. 2006;17:943–955.

44. Browaeys R, Saelens W, Saeys Y. NicheNet: modeling intercellular communication by linking ligands to target genes. *Nat Methods*. 2020;17:159–162.